MOLECULAR AND CELLULAR BIOLOGY, July 2006, p. 5106–5119 Vol. 26, No. 13
0270-7306/06/$08.00+0 doi:10.1128/MCB.00101-06

Receptor Protein Tyrosine Phosphatase γ Is a Marker for Pyramidal Cells and Sensory Neurons in the Nervous System and Is Not Necessary for Normal Development

Smaragda Lamprianou,[1] Nathalie Vacaresse,[1] Yoshihisa Suzuki,[2] Hamid Meziane,[3] Joseph D. Buxbaum,[4] Joseph Schlessinger,[2] and Sheila Harroch[1]*

Institut Pasteur, Department of Neuroscience, 25 Rue du Dr. Roux, 75724 Paris, France[1]; Yale University School of Medicine, Department of Pharmacology, P.O. Box 208066, New Haven, Connecticut 06520-8066[2]; Mouse Clinical Institute, 67404 Illkirch Cedex, Strasbourg, France[3]; and Mount Sinai School of Medicine, Departments of Psychiatry, Neuroscience, and Geriatrics and Adult Development, One Gustave Levy Place, New York, New York 10029[4]

Received 17 January 2006/Returned for modification 26 February 2006/Accepted 15 April 2006

In order to gain insight into the biological role of receptor protein tyrosine phosphatase γ (RPTPγ), we have generated RPTPγ-null mice. RPTPγ was disrupted by insertion of the β-galactosidase gene under the control of the RPTPγ promoter. As the RPTPγ-null mice did not exhibit any obvious phenotype, we made use of these mice to study RPTPγ expression and thus shed light on potential biological functions of this phosphatase. Inspection of mouse embryos shows that RPTPγ is expressed in a variety of tissues during embryogenesis. RPTPγ is expressed in both embryonic and adult brains. Specifically, we detected RPTPγ expression in cortical layers II and V and in the stratum pyramidale of the hippocampus, indicating that RPTPγ is a marker for pyramidal neurons. Mixed primary culture of glial cells showed a lack of expression of RPTPγ in astrocytes and a low expression of RPTPγ in oligodendrocytes and in microglia. Interestingly, RPTPγ expression was detected in all sensory organs, including the ear, nose, tongue, eye, and vibrissa follicles, suggesting a potential role of RPTPγ in sensory neurons. An initial behavioral analysis showed minor changes in the RPTPγ-null mice.

The phosphorylation of proteins on tyrosine residues is essential for transmission of signals for cell growth, proliferation, and differentiation. Phosphorylation depends on a regulated balance between the activities of protein tyrosine kinases and protein tyrosine phosphatases (PTP). While the roles and the mechanisms of action of tyrosine kinases are well characterized, our present understanding of tyrosine phosphatases is less developed.

PTP are classified into two groups, one comprising cytoplasmic and the other transmembrane, or receptor type (receptor protein tyrosine phosphatases [RPTP]), proteins. Seven different classes of RPTP have been defined, based primarily upon variations in the extracellular domain (reviewed in references 2 and 9). RPTP have one or more intracellular catalytic domains with a conserved cysteine at the active site, a transmembrane region, and an extracellular domain. We have focused our studies on RPTPγ, a receptor-type PTP containing an extracellular carbonic anhydrase domain, a fibronectin type III domain, and a spacer domain (1). RPTPγ is representative of a subfamily of RPTP that includes RPTPζ (also designated RPTPβ). As is the case for RPTPζ, several isoforms have been described for RPTPγ (19). RPTPγ-B lacks 29 amino acids in a cytosolic helix-turn-helix like motif in the juxtamembrane position compared to the full-length RPTPγ-A isoform. RPTPγ-C contains only one phosphatase domain, while RPTPγ-D is a soluble isoform and has lost all phosphatase activity.

Very few studies have reported on the biological function of RPTPγ. Overexpression of RPTPγ-A in the neuronal PC12D cell line prevented neurite outgrowth upon nerve growth factor (NGF) treatment (20). Both interleukin 1β and tumor necrosis factor upregulate RPTPγ mRNA in astrocytoma cell lines, suggesting a potential role for RPTPγ in the development of inflammatory diseases of the brain (18). RPTPγ maps to chromosome 3p14.2, a locus frequently deleted in lung, renal, and early-stage breast tumors, and was thought to be a target of a translocation at 3p14 in renal cell carcinoma (10, 11). However, other candidate tumor suppressor genes have been identified in the same chromosomal area. Still, a point mutation of RPTPγ has been detected recently in colon cancer (27) and reduced expression of RPTPγ has been observed in gastric cancer tissues (28), implying a potential role in tumor suppression. The lack of tools such as specific antibodies and genetically manipulated mice models has hindered the elucidation of the roles of RPTPγ. Moreover, reports on RPTPγ to date suggest species differences, and the exact cell types expressing RPTPγ still await determination.

We generated an RPTPγ knockout/β-galactosidase (β-Gal) knockin mouse and characterized expression of RPTPγ and behavior of these animals. We demonstrate that RPTPγ is expressed during embryogenesis and in adult mice in a variety of tissues. RPTPγ is also expressed in the brain, with strong expression in pyramidal and sensory neurons. Finally, we demonstrate that RPTPγ-null mice did not show any obvious phenotype and exhibited minor behavioral changes.

* Corresponding author. Mailing address: Institut Pasteur, Department of Neuroscience, 25 Rue du Dr. Roux, 75724 Paris, France. Phone: (33)140613424. Fax: (33)140613421. E-mail: sharroch@pasteur.fr.

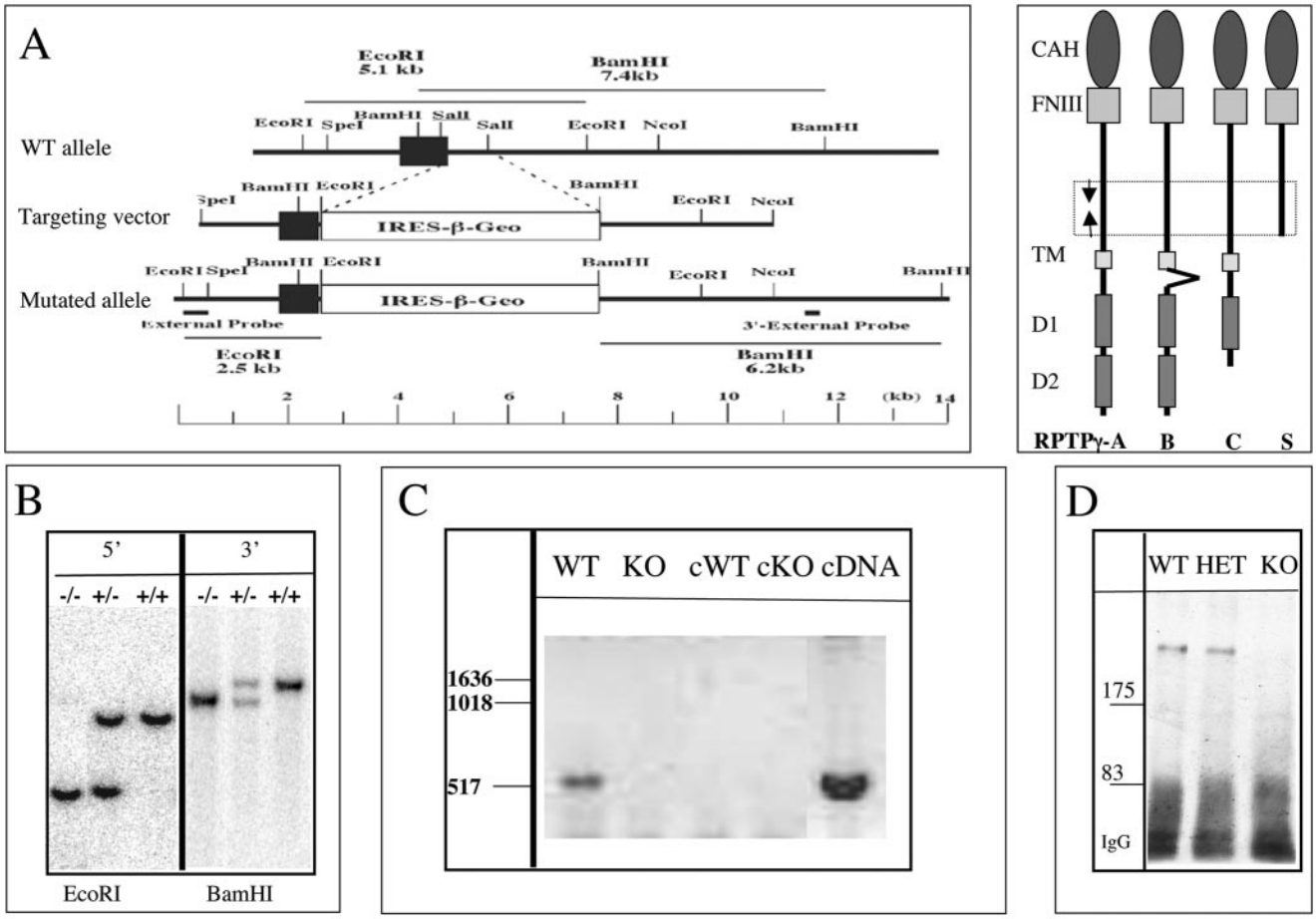

FIG. 1. Generation of RPTPγ knockout-LacZ transgenic mice. (A) Structures of the wild-type (WT) RPTPγ mouse gene and of the targeting vector used for generating heterozygous and knockout mice. IRES, internal ribosome entry site; β-Geo, β-Gal/neomycin resistance fusion protein; CAH, carbonic anhydrase domain; FNIII, fibronectin type III domain; TM, transmembrane domain. (B) Southern blot of genomic DNA of wild-type (+/+), heterozygous knockout (+/−), and homozygous knockout (−/−) mice, using the 5′ and 3′ probes indicated in panel A. (C) Reverse transcriptase PCR analysis using total RNA prepared from WT and knockout (KO) brains. PCR was carried out on RNA incubated with (WT and KO) or without (cWT and cKO) reverse transcriptase and on purified RPTPγ cDNA (cDNA). Primers were chosen to amplify all RPTPγ isoforms (arrows on scheme). (D) Immunoprecipitation and immunoblotting for RPTPγ in extracts from WT, heterozygous (HET), and KO brains. Immunoprecipitation and immunoblotting were carried out using RPTPγ antibodies directed against the C terminus of RPTPγ (D2 domain on scheme). IgG from the immunoprecipitation is indicated. In panels C and D, base pair numbers and molecular weights, respectively, are noted at the left of blots.

MATERIALS AND METHODS

Generation of mice with a disruption of RPTPγ. The construction of the transgene and the RPTPγ-β-Gal knockin mouse gene is shown in Fig. 1. To generate RPTPγ-null mice, an internal ribosome entry site–β-Gal–neomycin–poly(A) cassette was inserted into 3′ to exon 1. Linearized vector was electroporated into W4 embryonic stem (ES) cells, and homologous recombination was confirmed by the presence of a 2.5-kb EcoRI fragment (in addition to the native 5.2-kb fragment) with Southern blot analysis using a 5′ probe and the presence of a 6.2-kb BamHI fragment using a 3′ probe. Two correctly targeted ES cell clones were used in embryo aggregation to generate germ line chimeras. This transgene results in the promoter of RPTPγ driving the expression of the fusion protein between β-Gal and neomycin instead of RPTPγ. Wild-type and heterozygous or homozygous animals were either maintained as pure 129SvEv stock or used at a third-generation backcross to C57BL/6 for behavioral analysis.

Reverse transcription and PCR. Total RNA was prepared from RPTPγ-deficient and wild-type brains. RNA (1 μg) of each genotype was incubated with or without the Moloney murine leukemia virus reverse transcriptase (Roche). PCR using primers located on the extracellular domain of RPTPγ (forward primer, 5′-GCACCGAGCAAGGACAGCGAG-3′; reverse primer, 5′-GAGGA GGACGAGGCACACAAG-3′) was then carried out.

RPTPγ antibodies. Rabbit antibodies against RPTPγ were generated against glutathione *S*-transferase (GST) fusion protein containing the second phosphatase domain (amino acids 1120 to 1445). Affinity purification of serum was performed using a protein A-Sepharose column. Antibodies directed against the GST moiety were then removed by passing the affinity-purified antibodies over a Sepharose-GST column.

Western blotting and immunoprecipitation. One hundred micrograms of total brain lysates was immunoprecipitated using the RPTPγ antibodies. Following electrophoresis and blotting, the membrane was blotted with a 1/500 dilution of the RPTPγ antibodies and revealed by enhanced chemiluminescence.

In situ hybridization. In situ hybridization was performed with an antisense RNA probe coding for the N terminus of the carbonic anhydrase domain of RPTPγ (amino acids 1 to 832) transcribed by T3 polymerase (Roche). Embryos at different stages were frozen with an isopentane solution and sectioned at 16 μm with a cryostat. Slides were fixed in 4% paraformaldehyde (PFA) for 15 min, washed in phosphate-buffered saline (PBS), and then acetylated in a solution containing 1.3% triethanolamine (Sigma), 0.2 M HCl, and 0.25% acetic anhydride for 10 min. The slides were then washed in PBS, transferred into prehybridization buffer (50% formamide [Sigma], 5× SSC [1× SSC is 0.15 M NaCl plus 0.015 M sodium citrate], 5× Denhardt's solution, 250 μg/ml yeast tRNA

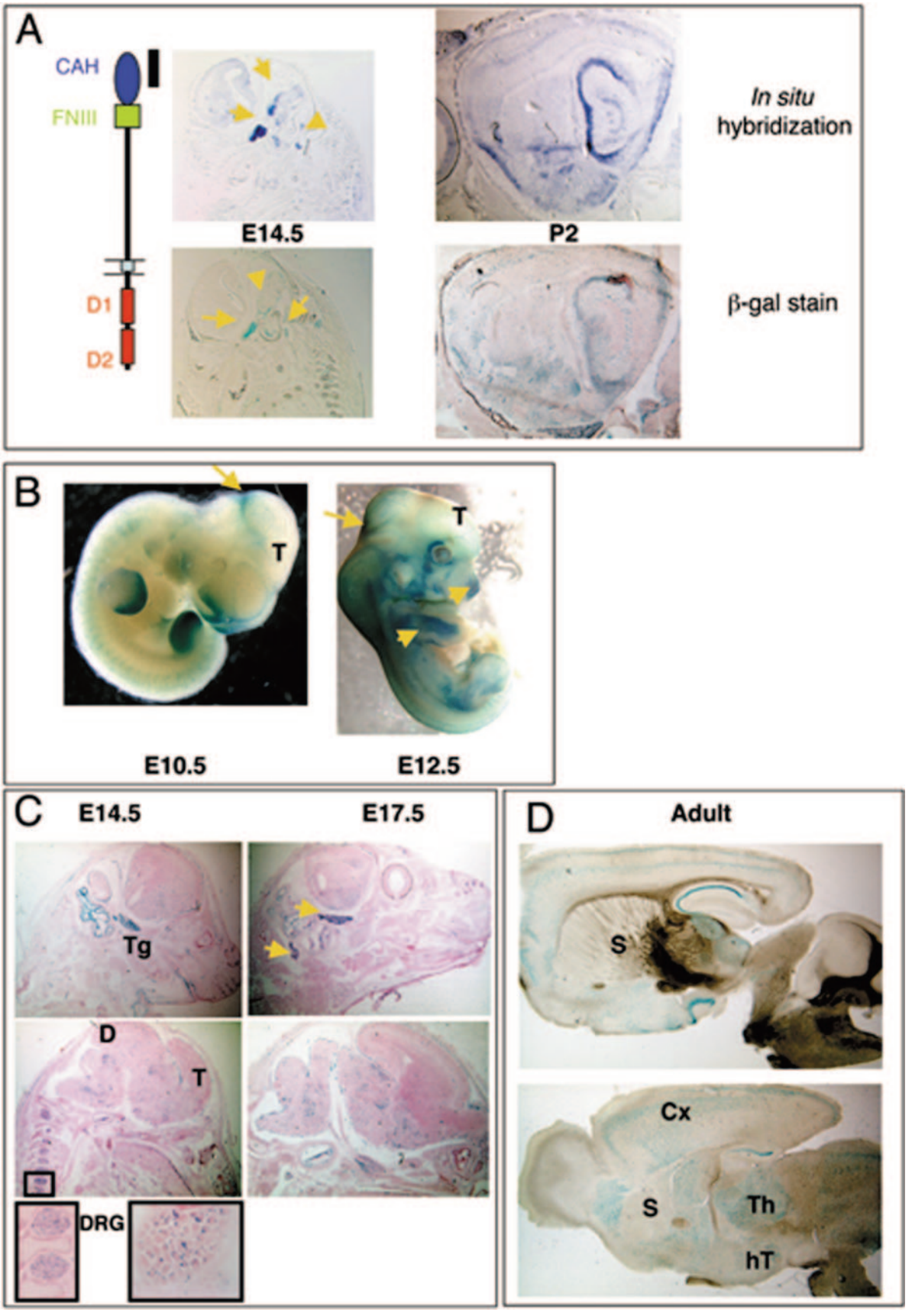
A
CAH
FNIII
D1
D2
E14.5
P2
In situ hybridization
β-gal stain
B
T
T
E10.5
E12.5
C
E14.5
E17.5
Tg
D
T
DRG
D
Adult
S
Cx
S
Th
hT

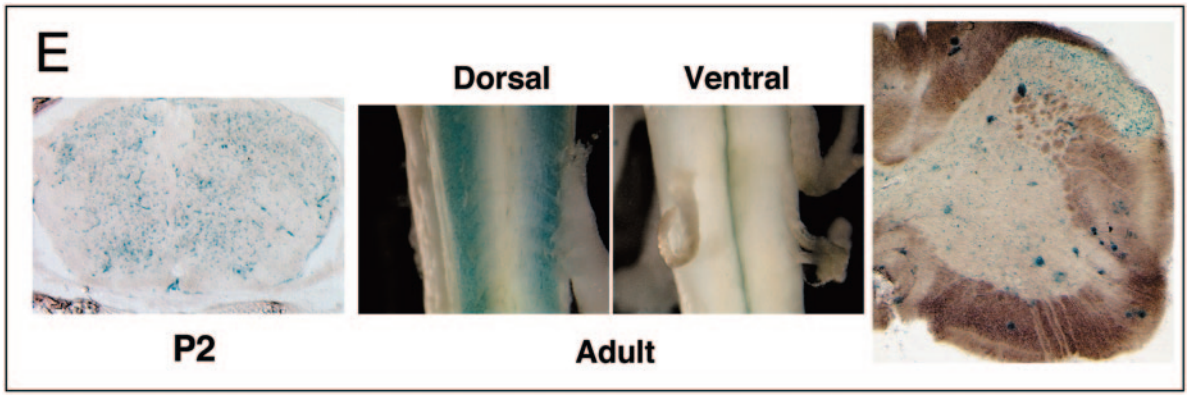

FIG. 2. Expression of RPTPγ in the CNS. (A) Comparison between in situ hybridization (top) by use of an extracellular probe (indicated by the black bar in the scheme on the left) and β-Gal staining (bottom) of consecutive sagittal sections from either an E14.5 heterozygous embryo (left) or a P2 heterozygous brain (right), demonstrating RPTPγ localization. The arrows in the left panels highlight examples of structures stained by both methods. CAH, carbonic anhydrase domain; FNIII, fibronectin type III domain. (B) Whole-mount β-Gal staining at embryonic stages E10.5 and E12.5. Arrows point to the isthmus. Arrowheads indicate the nose and forelimb. (C) Sagittal sections of E14.5 and E17.5 embryos. Arrows indicate the trigeminal ganglia (top) and the left inferior ganglion of the glossopharyngeal (IX) nerve. Higher magnification of the DRG is shown in the two insets. (D) Sagittal sections of adult brains. (E) Staining of P2 (coronal section) and adult (whole mount) spinal cords. Cx, cortex; D, diencephalon; hT; hypothalamus; S, striatum; T, telencephalon; Tg, trigeminal ganglia; Th, thalamus.

[Sigma], and 500 μg/ml herring sperm DNA [Roche]) for 2 h at 70°C, and incubated for 18 h at 72°C in the same solution with the probe. Slides were successively washed in 0.2× SSC, solution B1 (0.1 M Tris, pH 7.5, 0.15 M NaCl), and solution B2 (solution B1 enriched with 10% of heat-inactivated normal goat serum [NGS]) for 1 h at room temperature. Slides were then incubated with solution B2 containing alkaline phosphatase-conjugated antibody (Roche) at 1/2,500 overnight at 4°C. On the following day, slides were washed in solution B3 (0.1 M Tris, pH 9.5, 0.1 M NaCl, 50 mM $MgCl_2$, 0.25 mg/ml of levamisole [Sigma], and 0.1% Tween 20 [Sigma]) and incubated in B3 solution containing 4.5 μl/ml of nitroblue tetrazolium stock solution (75 mg/ml in 70% dimethylformamide [Roche]) and 3.5 μl/ml of 5-bromo-4-chloro-3-indolylphosphate (50 mg/ml in 70% dimethylformamide [Roche]). Slides were then dried and covered with a coverslip in Mowiol medium.

Expression of β-galactosidase in vivo. Mice or embryos were either directly frozen at −80°C or perfused in 2% PFA, 0.2% glutaraldehyde, 5 mM EGTA, and 2 mM $MgCl_2$. Cryostat/vibratome sections (10 to 20 μm) were fixed and incubated in X-Gal solution (1× PBS, 5 mM EGTA, 2 mM $MgCl_2$, 0.5 mg/ml 5-bromo-4-chloro-3-indolyl-β-D-galactopyranoside [X-Gal], 10 mM potassium ferricyanide, and 10 mM potassium ferrocyanide) at 37°C. Slides were counterstained with 0.5% eosin or 1% neutral red.

Immunohistochemistry. Sections stained with β-Gal were fixed in 100% ethanol, washed in 0.1 M sodium phosphate buffer, pH 7.4, and incubated overnight at 4°C in solution A (bovine serum albumin 3%, NGS 3% in PBS) with anti-glial fibrillary acidic protein (GFAP) and anti-NeuN antibodies. After being washed, slides were incubated with secondary antibodies, Hoechst stained, and mounted. For timing experiments, sections were labeled with β-Gal and then fixed in acetone at −20°C and treated for bromodeoxyuridine (BrdU) staining as described previously (25). Rabbit anti-GFAP (Dako) and mouse immunoglobulin G1 (IgG1) anti-NeuN (Chemicon) were used at 1/200. Mouse IgG1 anti-BrdU (Becton Dickinson) was used at 1/100. All secondary antibodies were used at 1/200. For cellular morphology experiments, sections of injected brains with dextran-biotin were first incubated with streptavidin-Cy3 (1/2,000; Jackson) and Hoechst in 5% NGS–0.1% Triton X-100 and then incubated with β-Gal solution.

Primary culture of glial cells. Newborn (P0) heterozygote cortices were dissociated in a papain solution containing L-cysteine (0.48 mg/ml; Sigma), DNase I (100 μg/ml; Sigma), and papain (100 μl/ml; Worthington) for 20 min at 37°C. Washed cells were plated onto poly-D-lysine-coated flasks in Dulbecco's modified Eagle's medium containing 15% heat-inactivated fetal calf serum. Medium was changed twice a week. Two weeks after plating, microglial cells and oligodendrocyte progenitors were recovered by differential shaking. The remaining cells (astrocytes) were dissociated with trypsin. Oligodendrocytes were purified of residual astrocytes by differential adhesion. Purified microglia, astrocytes, or oligodendrocyte progenitors were plated on polyornithine-coated coverslips overnight, fixed, and incubated in β-Gal solution for 24 h at 37°C.

Timing experiments. Pregnant females were injected with BrdU (50 mg/kg of animal weight) at 13.5 and 16.5 days of pregnancy, using the time of detection of a vaginal plug as 0.5 days. Twenty days after birth, pups were sacrificed and were stained for BrdU and β-Gal.

Dextran-biotin injections. Mice were placed in a stereotaxic apparatus and injected unilaterally with dextran-biotin 10,000 (Molecular Probes) in the somatosensory cortex. Two days later, mice were sacrificed and perfused. The brains were briefly postfixed and then cryoprotected in 30% sucrose and cut on a freezing microtome to 40-μm sections.

Histology of the brain and spinal cord. RPTPγ-deficient and wild-type mice were perfused with sodium sulfite solution followed by 4% PFA. Paraffin sections (5 μm thick) of the brains and spinal cords were labeled using the Timm staining protocol (5) or stained with hematoxylin and eosin.

Behavioral analyses. Male wild-type and knockout littermates were used for behavioral analyses. Animals were about 13 weeks old at the beginning of testing. Animals were housed in groups of two or three mice and maintained in a room with controlled temperature and light under a 12-h to 12-h light-dark cycle at 21 to 22°C, with food and water available ad libitum. Behavioral phenotyping was carried out over a period of 5 weeks, with 24 to 48 h between tests. Phenotyping included assessments of general health and basic sensory-motor functions, as well an extended test battery designed to investigate a wide range of brain functions, including basic sensory-motor abilities, circadian activity, anxiety, depression, information processing, learning and memory, and susceptibility to epileptic seizures. Detailed methods are described below. All experiments were carried out in accordance with the European Communities Council Directive of 24 November 1986.

Detailed methods of behavioral analyses. To assess general health and basic sensory-motor functions, each mouse was transferred into a new cage and careful preliminary observations using a modified version of standard procedures for behavioral phenotyping of genetically modified mice were performed (Irwin screen [7b] and SHIRPA [7a]). General health was evaluated by measuring body weight, body temperature, and overt behavioral signs. Sensory functions were evaluated by measuring or scoring visual ability, audition, olfaction, tactile perception, and vestibular function. Visual ability was assessed as orientation responses to an object (a white cotton swab) being moved in each peripheral visual field at a distance of 5 cm. Auditory function was evaluated by scoring Preyer and startle reflexes (pinna flicking backwards, startle) to 90-dB click noise of 20-kHz frequency and acoustic startle. Olfaction was evaluated by scoring olfactory exploration of an object (a cotton swab) presented in front of the animal's muzzle. Tactile perception was evaluated by scoring the mouse reaction to tail or toe pinch. Motor functions were evaluated by the use of specific tests, including rotarod, string, and grip tests, as well as by measure of spontaneous locomotor activity. For the rotarod test, mice were given three trials separated by 5- to 10-min intervals during which the speed of rotation accelerated from 4 to 40 rpm in 5 min. The string test involved a wire stretched horizontally 40 cm above a

table. Testing consisted of three consecutive trials separated by 10-min intervals. On each trial the forepaws of the animal were placed on the thread, and the latency the animal took to catch the wire with its hindpaws was recorded (13a). For the grip test, each mouse was subjected to two trials separated by 5- to 10-min intervals. When the animal was holding the grid with its all paws, it was slowly moved backwards until it released it. A dynamometer recorded the maximal strength generated. Pain sensitivity was measured by tail flick, hot plate, and shock threshold. Tail flick was assessed in three consecutive trials with an interval of about 1 min (performed at different sites of the tail). For each trial, the tail of the animal was placed under a heat source. The time taken by the animal to flick its tail was recorded (cutoff, 20 s). For the hot plate test, mice were placed into a glass cylinder on a hot plate adjusted to 52°C and the latency of the first reaction (licking, moving the paws, or little leaps) was recorded. The test was ended if the mouse failed to show any sign within 30 s in order to avoid potential tissue injury. For shock threshold, mice were placed in a fear-conditioning chamber and allowed to habituate for 30 s. Foot shock was then manually applied for 1 s, and behavioral responses were noted. Shock levels began at 0.05 mA and increased in 0.05-mA steps with 30-s intervals between shocks, until both flinch (any detectable response) and vocalizations were induced. After this point, shocks were increased in 0.1-mA steps until a jump was induced. A 1-mA cutoff was employed in this test.

Circadian activity was analyzed. Spontaneous locomotor activity was measured using boxes equipped with infrared analyzers allowing measurement of ambulatory locomotor activity and rears. Mice were tested for 32 h in order to measure habituation to the apparatus as well as nocturnal and diurnal activities.

Anxiety and depression measures were carried out and included light-dark exploration, open field, and tail suspension. For light-dark exploration, an apparatus consisting of dark and illuminated chambers with an interconnecting dark tunnel was used (Imetronic). The test was initiated by placing the mouse in the dark chamber. The latency to enter and amount of time spent in the lit chamber, the number of transitions between the two chambers, and locomotor activity and rearings in each chamber were recorded over a 5-min period. For the open field test, mice were tested in automated open fields (Panlab, Barcelona, Spain), placed in a room homogeneously illuminated at 150 lux. The open-field arena was divided into central and peripheral regions. Mice were placed in the periphery of the open field and allowed to explore freely for 30 min, with the experimenter out of the animal's sight. The distance traveled, the number of rearings, and time spent in the central and peripheral regions were recorded over the test session. The latency and number of crosses into as well as the percent time spent in center area were used as indices of emotionality/anxiety. For tail suspension, mice were tested in an automated tail suspension device (MED Associates Inc., St. Albans, Vt.). Immobility time was monitored through 6-min period in blocks of 2-min intervals. Latency to first immobilization was also determined.

Sensorimotor gating was then analyzed. Acoustic startle reactivity and prepulse inhibition of startle were assessed in a single session using standard startle chambers (SR-Lab Startle Response System; San Diego Instruments). Ten different trial types were used: acoustic startle pulse alone (120 dB); eight different prepulse trials in which either 70-, 80-, 85-, or 90-dB stimuli were presented alone or preceding the pulse; and finally one trial (NOSTIM) in which only the background noise (65 dB) was presented to measure the baseline movement in the Plexiglas cynlinder. In the startle pulse or prepulse-alone trials, the startle reactivity was analyzed, while in the prepulse plus startle trials the amount of prepulse inhibition was measured and expressed as a percentage of the basal startle response.

Learning and memory were assessed in a Y maze and in a Pavlovian fear-conditioning model. The Y maze consisted of three arms (40 by 9 by 16 cm) placed 120° from each other. Each arm had walls with unique patterns. Mice were placed at the end of one arm with the head directed to the walls and allowed to explore the apparatus freely for 5 min. Alterations were operationally defined as successive entries into each of the three arms. Percent spontaneous alternation performance was defined as the ratio of actual (total alternations) to possible alternations (total arm entries − 2) × 100. We scored alternate-arm returns and same-arm returns for each animal in order to assess aspects of attention within spontaneous working memory (26a). Total entries and the latency to exit the starting arm were also scored as an index of ambulatory activity and emotionality in the Y maze, respectively. For Pavlovian fear conditioning, four identical polymodal operant chambers (Coulbourn Instruments, Allentown, PA) were used. Each chamber (18.5 by 18 by 21.5 cm) consisted of aluminium side walls and Plexiglas rear and front (the door) walls. A loudspeaker and a bright light were inserted in the opposite side walls and constituted the sources of the cues during conditioning and cue testing. The general activity of animals was recorded through the infrared cell placed at the ceiling of the chambers and was directly recorded on a computer using Graphic State software (Coulbourn). For conditioning, mice were allowed to acclimate for 4 min, and then a light/tone (10-kHz) conditioning stimulus (CS) was presented for 20 s and coterminated by a mild (1-s, 0.4-mA) footshock (US). Two minutes later another CS-US pairing was presented. Two minutes later, mice were returned to their home cages. Testing was performed 24 h following the conditioning session. Testing for the context was performed in the morning. The mouse was placed back into the same chamber that was used for the conditioning and allowed to explore for 6 min without presentation of the light/auditory CS. Testing for the cue was performed in the afternoon (about 5 h after the context testing). The contextual environment of the chambers was changed (wall color, odor, and floor texture). The mouse was placed in the new chamber, allowed to habituate for 2 min, and then presented with light/auditory cues for 2 min. This sequence was repeated once again.

Sensitivity to pentylene-tetrazol-induced seizures was then analyzed. Pentylene tetrazol was dissolved in saline (0.9% NaCl) and injected intraperitoneally at 50 mg/kg of body weight. Immediately after injection, the mouse was placed into a new cage and observed for at least 20 min. The seizure profile (myoclonic, clonic, or tonic) as well as the latency and duration of clonico-tonic seizure was scored.

For quantitative parameters showing normal distribution, data were analyzed using an unpaired Student *t* test or repeated-measure analysis of variance with one between factor (genotype) and one within factor (time). Qualitative parameters (e.g., seizure profile and some of clinical observations) were analyzed using a C^2 test. The level of significance was set at $P < 0.05$.

RESULTS

Generation of RPTPγ knockout mice. Since RPTPγ functions in ES cells (24), we generated β-Gal knockin/RPTPγ knockout mice, with the RPTPγ promoter controlling expression of a β-Gal/neomycin resistance fusion protein (Fig. 1A). Southern blot analyses using both the 5′ probe and the 3′ probe demonstrated appropriate homologous recombination (Fig. 1B). Northern blot analysis, using a probe corresponding to the region encoding the RPTPγ membrane-proximal phosphatase domain, revealed no detectable levels of RPTPγ mRNA in the homozygous mutant brain (data not shown). To ensure that all four isoforms of RPTPγ were deleted, PCR analysis with primers that amplify all four isoforms was carried out (Fig. 1C). Appropriately sized product was observed with RNA derived from the wild-type brain but not the knockout brain. Finally, no RPTPγ protein was detected in brains of RPTPγ-null mice by immunoblot analysis with anti-RPTPγ antibodies developed against the C terminus (D2 domain) of RPTPγ (Fig. 1D). These antibodies recognize RPTPγ-A and RPTPγ-B. These results confirm the generation of an RPTPγ-null animal.

RPTPγ knockout mice appeared grossly normal at birth. In an analysis of 263 pups from multiple matings of heterozygous knockout mice, 66 were wild-type mice, 147 were heterozygous mice, and 50 were RPTPγ-null mice. The slight reduction in the number of knockout animals (19.4% of the total) was not statistically significant.

RPTPγ is expressed in the central nervous system (CNS). The introduction of β-Gal knockin under the control of the RPTPγ promoter permits a detailed analysis of the expression of patterned RPTPγ. To first confirm that β-Gal expression corresponds to RPTPγ localization, we compared the staining obtained by in situ hybridization with a probe for the N-terminal domain of RPTPγ (present in all RPTPγ isoforms) to β-Gal staining of sagittal sections from both a heterozygous embryo at embryonic day 14.5 (E14.5) and a heterozygous brain at day 2 after birth (P2). The patterns of

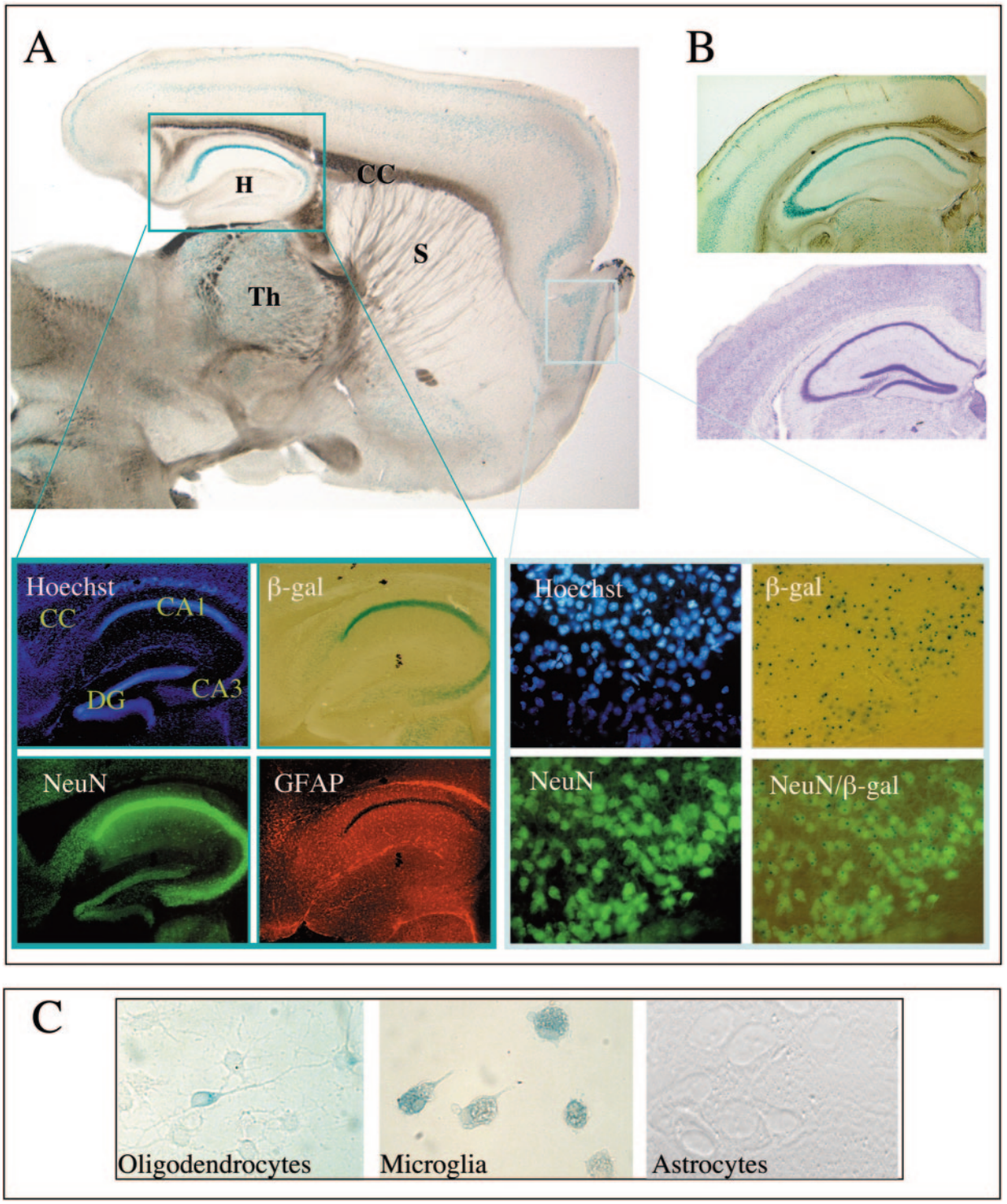

FIG. 3. Laminar expression of RPTPγ in the brain. (A) Sagittal section of adult brain. Coronal sections of the hippocampus (left insets) or the piriform cortex (right insets). H, hippocampus; Th, thalamus; S, striatum; CC, corpus callosum; DG, dentate gyrus. (B) Coronal sections of the hippocampus stained for β-Gal (top) and Nissl (bottom). (C) Staining of primary cultures of glial cells. Left, purified oligodendrocyte progenitor cells; middle, purified microglia; right, purified astrocytes.

expression appeared identical (Fig. 2A), demonstrating that β-Gal expression in these mice is a reliable indicator of RPTPγ expression.

During embryonic development, β-Gal activity was first localized in the somites and the nose at E10.5 (Fig. 2B). At both E10.5 and E12.5, distinct labeling of the vascular system of the brain was observed (Fig. 2B). The isthmus, a constriction that separates the mesencephalon from the telencephalon, was

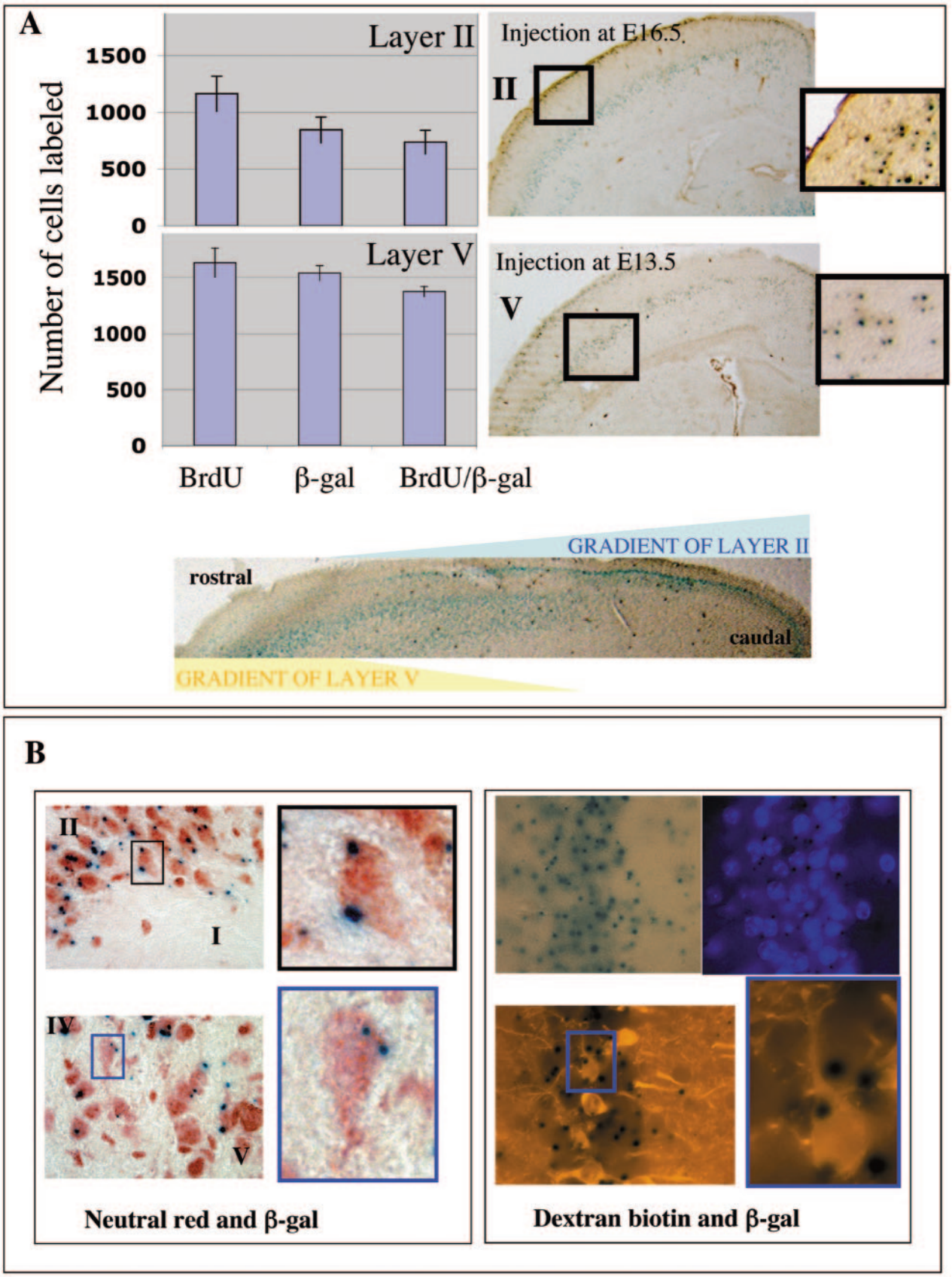
A
Layer II
Layer V
Number of cells labeled
1500
1000
500
0
BrdU
β-gal
BrdU/β-gal
Injection at E16.5
II
Injection at E13.5
V
GRADIENT OF LAYER II
rostral
caudal
GRADIENT OF LAYER V
B
II
I
IV
V
Neutral red and β-gal
Dextran biotin and β-gal

strongly labeled (Fig. 2B), but there was no labeling of cells in the neural tube (data not shown).

In serial sections of E14.5 and E17.5 embryos, we detected β-Gal in the diencephalon and mesencephalon, pons, and medulla oblongata and, later, in the telencephalon (Fig. 2C). The peripheral nervous system was also labeled, and we clearly detected strong expression of RPTPγ in dorsal root ganglia (DRG).

In the adult, most of the structures rich in neurons, including the cortex, the pyramidal fields (CA1, CA2, and CA3) of the hippocampus, the thalamus, and the hypothalamus, appeared positive for β-Gal. No β-Gal staining was detected in the striatum, the corpus callosum, or the subventricular zone (Fig. 2D), regions rich in glia. In the spinal cord, expression in neonates was seen in both the dorsal and ventral horns but was confined in the adult to the dorsal horns (Fig. 2E).

RPTPγ is expressed predominantly in neurons. The expression of RPTPγ corresponded closely to staining with cresyl violet, which labels the Nissl bodies of neurons (Fig. 3A and B). Further immunohistochemical studies using NeuN and GFAP as specific markers for nuclei of neurons and astrocytes, respectively, showed that cells expressing β-Gal were all NeuN positive in the hippocampus and in the piriform cortex, indicating that RPTPγ is strongly expressed in neuronal cells (Fig. 3A, insets). The strong expression in neurons may mask RPTPγ expression in other cell types. To address this point, primary cultures were prepared from cortices of newborn heterozygous RPTPγ knockout mice, and astrocytes, microglia, and oligodendrocytes were purified and examined for β-Gal expression. Microglia showed weak β-Gal expression after 12 h of incubation with substrate, while only a small fraction of the oligodendrocytes stained for β-Gal (Fig. 3C). No expression of RPTPγ was detected in astrocytes (Fig. 3C).

To determine which cortical layers express RPTPγ, we used a birth-dating method, administering BrdU to pregnant females at different stages of cortical neurogenesis. BrdU was injected at E13.5 and E16.5, the days of neurogenesis of the majority of neurons of layers V and II, respectively. After injections at E16.5, 87.1% of the BrdU-positive cells also contained β-Gal, and when injected at E13.5, 93% of the BrdU-positive cells were positive for β-Gal (Fig. 4A). This indicated that the RPTPγ is expressed in cortical layers II and V, two layers rich in pyramidal neurons. β-Gal expression levels in layers II and V appeared to vary across the anterior-posterior axis (increasing and decreasing gradients, respectively). To confirm expression in pyramidal cells, we injected dextran-biotin to retrogradely label pyramidal cells that have long projecting axons to the ipsilateral and contralateral cortices (Fig. 4B, right). Retrogradely labeled pyramidal cells showed β-Gal staining. In addition, neutral red counterstaining showed that cells with a pyramid-like morphology were positive for β-Gal (Fig. 4B, left).

TABLE 1. Behavioral and neurological testing

Parameter	Value (mean ± SD) for:	
	Wild-type mice ($n = 8$)	Knockout mice[b] ($n = 9$)
Body wt (g)	29.73 ± 0.52	26.08 ± 1.55
Body temp (°C)	38.36 ± 0.12	38.06 ± 0.18
Response to rotarod test[a] (s)	84.08 ± 10.94	50.22 ± 4.80**
Response to string test (s)	17.73 ± 6.07	39.13 ± 7.58*
Grip strength (g/g)	7.50 ± 0.43	7.64 ± 0.51
Response to tail flick test (s)	5.75 ± 0.37	4.60 ± 0.34*
Response to hot plate test (s)	7.24 ± 1.37	8.08 ± 0.82
Shock threshold		
Flinch (mA)	0.083 ± 0.003	0.082 ± 0.002
Vocalization (mA)	0.28 ± 0.06	0.36 ± 0.05
Sensory nerve conduction velocity (m/s)	66.2 ± 6.9	53.8 ± 5.0
Plantar muscle action		
M wave latency (s)	1.99 ± 0.07	1.95 ± 0.08
M wave amplitude (mV)	4.73 ± 0.61	5.4 ± 0.9
H wave latency (s)	5.14 ± 0.18	5.28 ± 0.14
H wave amplitude (mV)	1.16 ± 0.33	0.94 ± 0.15
Gastrocnemius muscle action		
M wave latency	0.87 ± 0.05	0.98 ± 0.06
M wave amplitude	32.2 ± 4.4	25.3 ± 3.1
Anxiety-related behavior in a light-dark test		
% Time in lit box	26.0 ± 4.6	21.4 ± 1.9
Latency to lit box (s)	41.0 ± 15.5	38.0 ± 8.5
No. of entries in lit box	12.6 ± 1.4	13.4 ± 1.2
No. of dark-light transitions	8.0 ± 1.0	10.3 ± 0.9
No. of rears in lit box	4.4 ± 1.8	4.8 ± 1.1
No. of rears in dark box	12.0 ± 1.5	12.8 ± 1.7
Tail suspension test		
Total time immobile (s)	114.7 + 30.7	70.1 + 18.8
Latency to first immobilization (s)	124.1 + 22.4	228.0 + 32.8*

[a] From 4 to 40 rpm in 5 min.
[b] *, $P < 0.05$; **, $P < 0.01$ (Student t test).

RPTPγ is expressed in sensory neurons and in sensory organs. In the CNS, β-Gal staining was observed to occur in major regions of sensory neurons, including nuclei of cranial nerves that innervate different sensory organs (including the ear, the tongue, the eye, the vibrissae, the olfactory bulb, and the nasal cavity). We detected clear expression of β-Gal in the ganglion cells of the retina, the cells of the glomerulus of the olfactory bulb, the surface of the tongue, the sensory and epithelial cells of the ear, the nasal cavity, and the follicles of the vibrissae (Fig. 5). Among the cranial nerves, we observed

FIG. 4. Expression of RPTPγ in pyramidal neurons. (A) Quantification of β-Gal- and BrdU-positive cells in adult mouse brain sections injected with BrdU at E13.5 or E16.5. (Bottom) β-Gal staining of a sagittal section of an adult cortex demonstrates opposing gradients of expression in layers II and V. Data represent means ± standard deviations of measurements from three animals, summing counts from 10 sections for each animal. (B) (Left) Neutral red and β-Gal labeling of pyramidal neurons from layers II and V, with higher magnifications boxed at right. (Right) β-Gal (upper left and lower left), Hoechst (upper right), and dextran-biotin (lower left) labeling of pyramidal neurons. The panel on the lower right is a higher magnification of that on the lower left, showing β-Gal staining colocalizing with dextran-biotin.

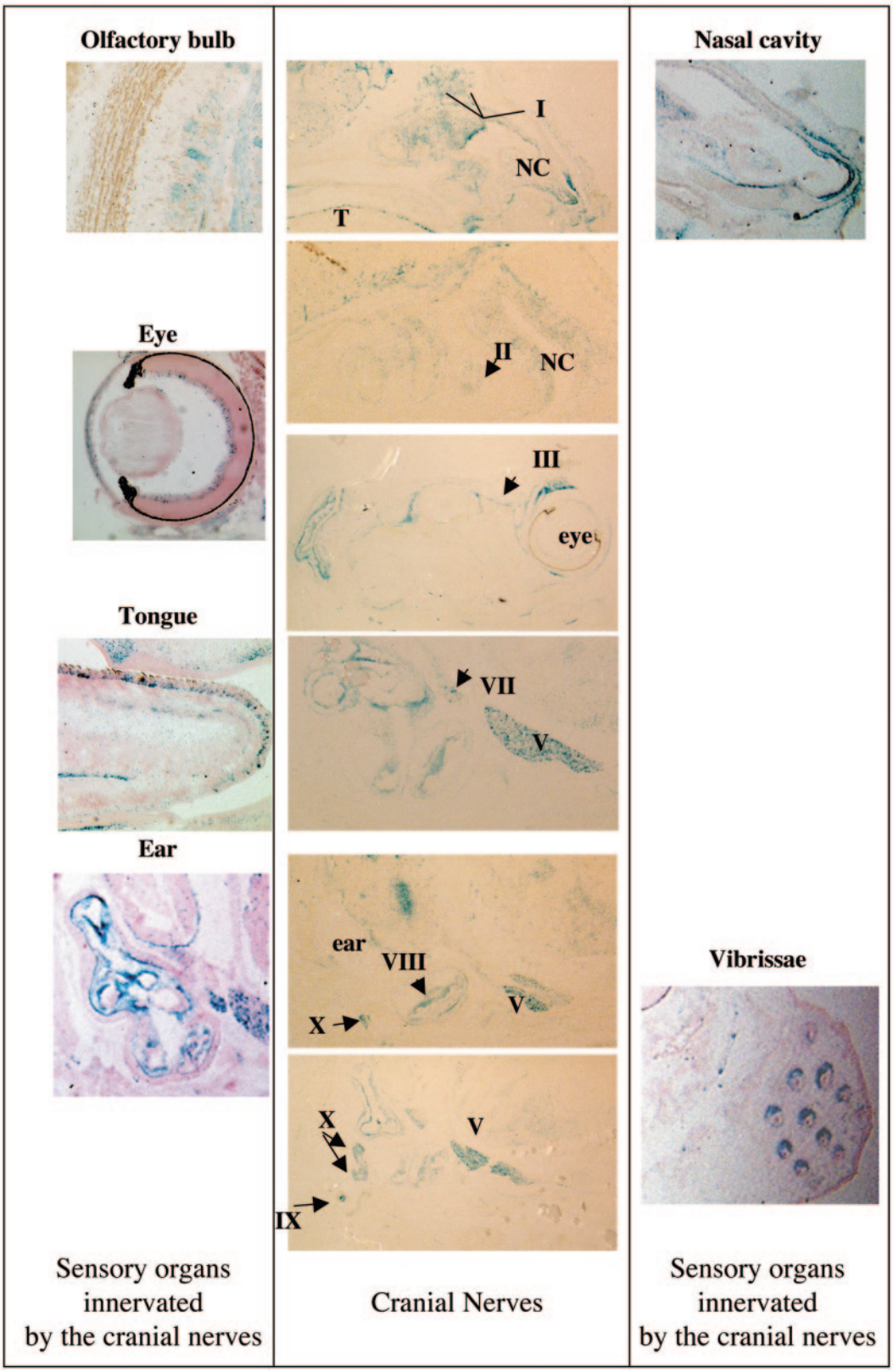

FIG. 5. Expression of RPTPγ in sensory neurons. (Left and right) β-Gal staining in sagittal sections of sensory organs innervated by cranial nerves, including olfactory bulb, eye, tongue, and ear, as well as nasal cavity wall and vibrissae. (Center) β-Gal staining of sagittal sections of head, showing labeling in cranial nerves I, II, III, V, VII, VIII, IX, and X. All sections are from an E14.5 embryo. T, tongue; NC, nasal cavity.

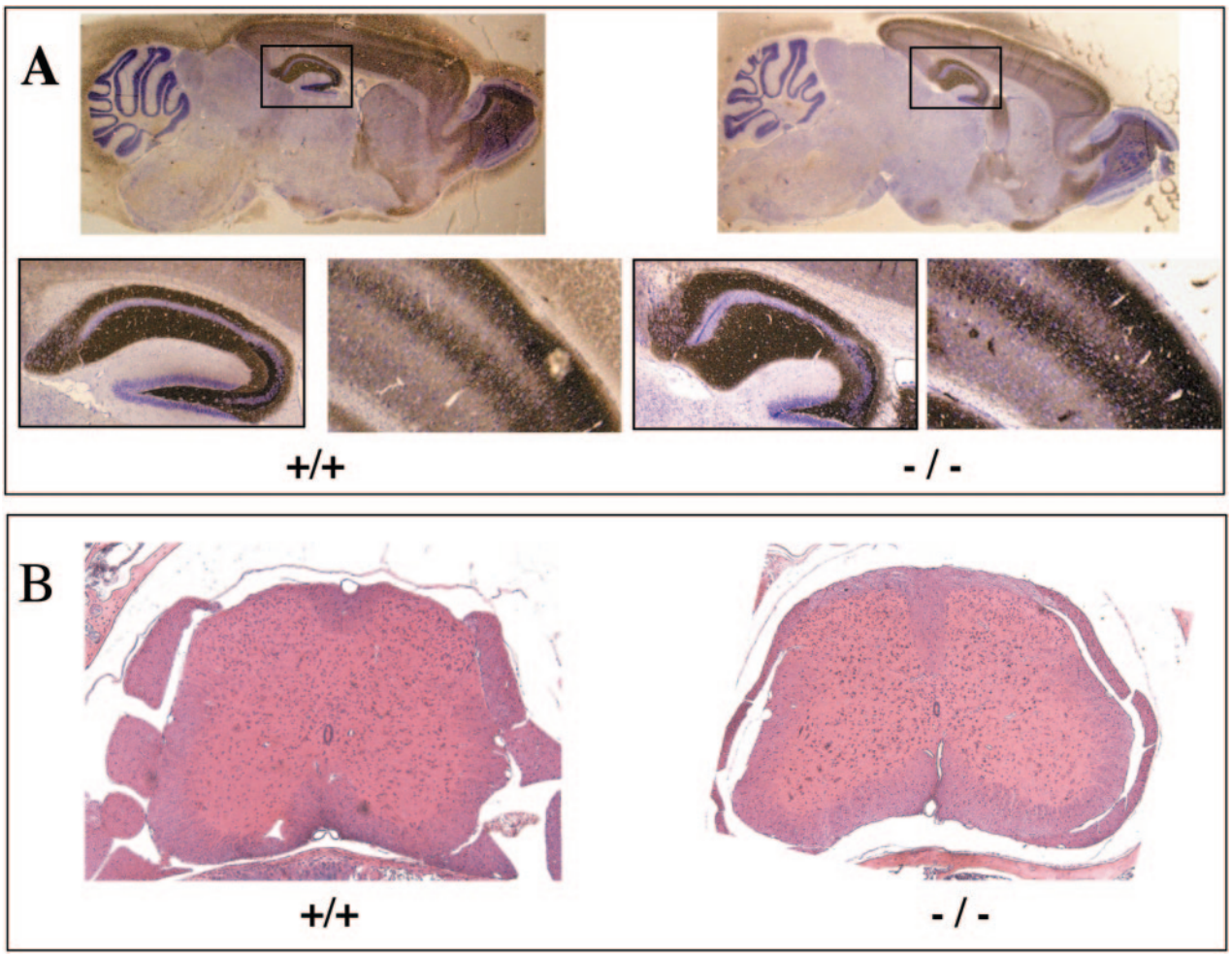

FIG. 6. Histology of the CNS in wild-type and knockout mice. (A) Timm staining of sagittal sections of adult brains from wild-type (+/+) and knockout (−/−) mice. The lower panels show enlargements of the hippocampus (left panels, sagittal) and the somatosensory cortex (right panels, coronal). (B) Hematoxylin and eosin staining of coronal sections of the spinal cords from wild-type (+/+) and knockout (−/−) mice.

labeling in cranial nerves I (olfactory), II (optic), III (oculomotor), V (trigeminal), VII (facial), VIII (vestibulocochlear), IX (glossopharyngeal), and X (vagus) (Fig. 5). These nerves correspond predominantly to sensory nerves, i.e., nerves that are exclusively sensory (I, smell; II, vision; and VIII, balance and hearing), as well as nerves that contain both sensory and motor fibers (V, VII, and IX). The particularly strong stain in the sensory organs suggests a potential role of RPTPγ in sensitive perception.

RPTPγ-null mice do not exhibit gross neuropathological abnormalities. The general morphology and histology of brains of 2-month-old RPTPγ-null mice appeared normal. To test whether RPTPγ-deficient mice had connectivity defects, we analyzed the pyramidal cells of the hippocampus, where RPTPγ is highly expressed, in relation to axonal projections, the mossy fibers. We used Timm staining, which specifically reveals mossy fibers and their synaptic extensions, and observed that hippocampal sections derived from wild-type and knockout mice were comparable (Fig. 6A). Since RPTPγ is expressed in cortical neurons, we compared the lamination and organization of the cortices. The number of cells and the organization were similar for wild-type and RPTPβ-deficient mice, demonstrating that RPTPγ is apparently not necessary for cortical-neuron migration (data not shown). Furthermore, the overall structure of the spinal cord appeared normal (Fig. 6B).

RPTPγ-deficient mice show modest behavioral changes. In terms of general health and sensory-motor functions, RPTPγ-null mice displayed slightly lower body weights than the wild-type littermates ($P = 0.05$) (Table 1), but all of the other traits of general health were normal. We investigated potential behavioral abnormalities resulting from RPTPγ gene disruption. For this purpose, heterozygous mice after three generations of backcross to C57BL/6 were mated, and wild-type and RPTPγ-null littermates (to control for genetic background) were tested in an extended test battery designed to investigate a wide range of brain functions, including basic sensory-motor abilities, circadian activity, anxiety, depression, information processing, learning and memory, and susceptibility to epileptic seizures.

RPTPγ-null mice also showed significant motor deficits, as revealed by the rotarod and string tests, although their muscle

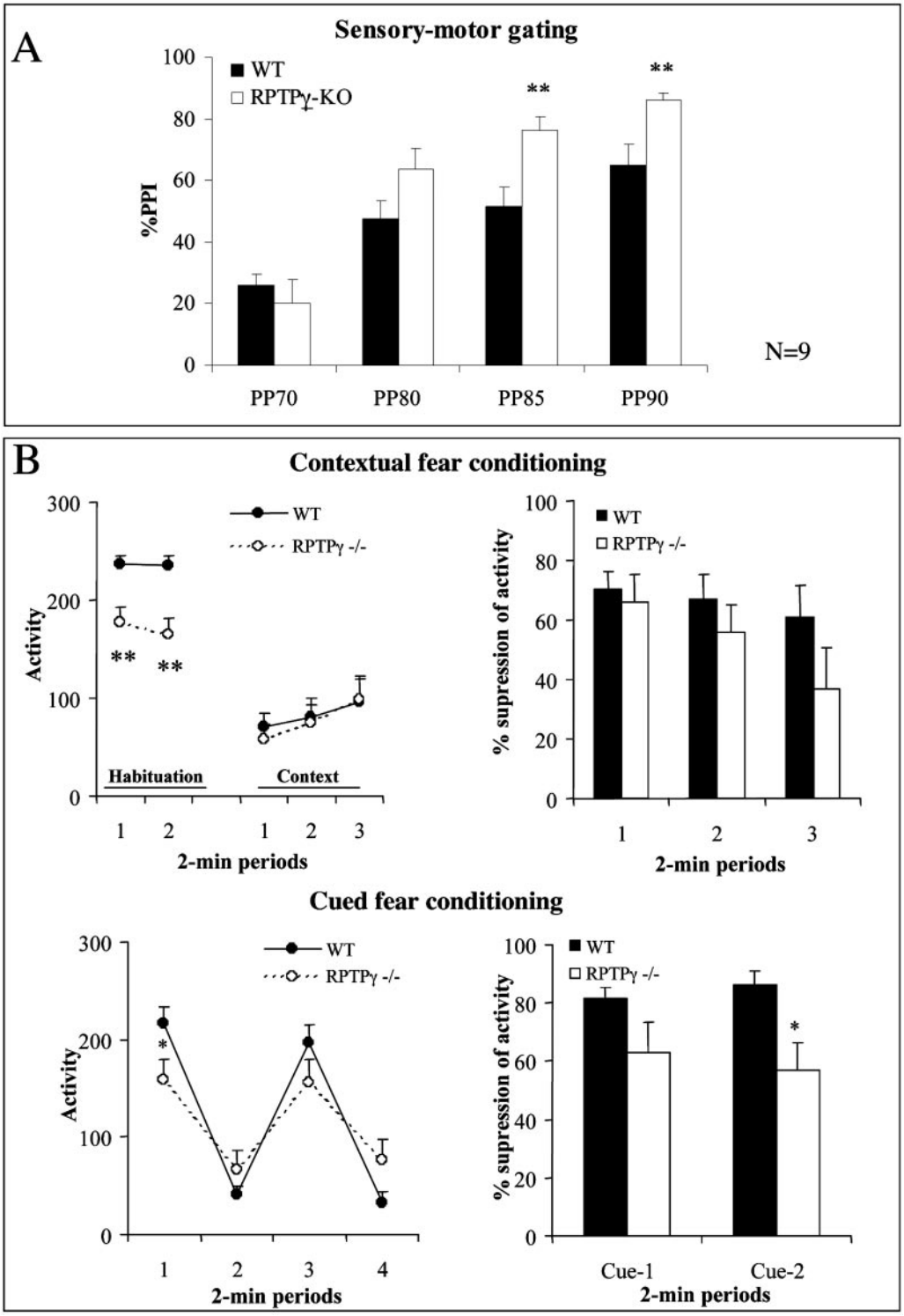

FIG. 7. Behavioral analyses of wild-type and knockout mice. (A) Sensory-motor gating with wild-type (WT, $n = 8$) and knockout (KO, $n = 9$) mice. Percent prepulse inhibition (PPI) of startle induced by a prepulse of the indicating intensities (in dB) is shown (e.g., PP70 indicates a prepulse of 70 dB). (B) Contextual and cued fear conditioning in WT and KO mice. *, $P < 0.05$; **, $P < 0.01$

strength was normal (Table 1). The knockout mice had reduced latencies in the tail flick test (Table 1); however, they had normal pain sensitivity in the hot-plate test and normal shock threshold. Electromyograph recording revealed that knockout mice had normal nerve conduction velocity and normal compound muscle action potentials evoked by sciatic nerve stimulation (Table 1).

In analyses of circadian activity, knockout mice showed nor-

mal circadian rhythm compared to their wild-type littermates, and for both genotypes spontaneous activity (ambulatory locomotion and rears) was markedly increased during the dark phase and reduced during the light phase (data not shown). Knockout mice also showed normal habituation to the novel environment, with both wild-type and knockout animals displaying a higher level of locomotor activity and rears at the beginning of testing, which rapidly decreased in the same way for both genotypes (data not shown).

In order to evaluate emotional behavior, animals were tested in different experimental paradigms known to trigger distinctive types of stress and anxiety. No differences in anxiety or exploratory measures between knockout and wild-type mice were detected with the light-dark test (Table 1). In the open-field test, locomotor activity and vertical exploratory activity were comparable between wild-type and knockout mice (data not shown). Anxiety-related parameters, such as the percentage of time spent in the central area, latency, and number of entries into this area, were also comparable between wild-type and knockout animals (data not shown). When animals were submitted to tail suspension tests, the total immobility times were not significantly different between the two genotypes (Table 1). However, the latency to the first immobilization of knockout mice was longer than that of the wild-type littermates (Table 1).

Mutant mice displayed normal startle response at 120 dB, and their reaction to the other acoustic stimuli used was also comparable to that of their wild-type littermates (data not shown). When the startling pulse was preceded by prepulses of increasing intensities, the amplitude of the startle response decreased significantly in both groups, reaching 65% and 86% at a 90-dB prepulse for wild-type and knockout animals, respectively (Fig. 7A). The knockout mice showed significantly improved prepulse inhibition [$F(1,15) = 5.59$, $P < 0.05$, repeated-measures analysis of variance (ANOVA)], particularly at higher prepulse intensities of 85 to 90 dB ($P < 0.01$; Student t test) (Fig. 7A).

In the Y-maze paradigm, no difference in ratio of spontaneous alternation was noted between knockouts (62.0 ± 2.7) and wild-type littermates (70.4 ± 5.9), indicating that working memory performances were not affected in the mutants. At the same time, knockouts were more active than wild types, displaying significantly higher numbers of arm entries (wild types, 18.9 ± 1.8; knockouts, 30.6 ± 2.2; $t15 = 4.06$, $P < 0.01$; student t test).

In the fear conditioning test, when exposed for the first time to conditioning cages, knockouts displayed significantly lower baseline levels of activity than did the wild-type littermates [$F(1,15) = 12.79$, $P < 0.01$] (Fig. 7B, upper left, "Habituation"). Conditioned stimulus-unconditioned stimulus pairing induced a significant decrease in activity, which differed between wild types and knockouts (data not shown) [group × period interaction: $F(3,45) = 25.51$, $P < 0.001$, repeated-measures ANOVA]. Indeed, the immediate response to foot shocks of wild-type animals was more pronounced and tendencies between the two genotypes were reversed, with wild-type mice being significantly less active than the knockouts [$F(1,15) = 6.80$, $P < 0.05$, repeated-measures ANOVA for the last two periods] (data not shown). When animals were reexposed in the same context 24 h after conditioning, both wild-type and knockout mice showed a significant decrease of activity compared to baseline [$F \geq 40.24$, $P < 0.001$, intragroup analysis for the last 2 min of habituation and the first 2 min of context] (Fig. 7B, upper left, "Context"). As can be seen from Fig. 7B, upper right, the levels of suppression of activity in both groups were comparable [$F(1,15) = 1.35$, not significant]. This indicates that both wild types and mutants remembered the context where they received the shock. When animals were placed in a new context, presentation of a conditioned stimulus alone induced a clear fear reaction in both wild types and knockouts that was reflected by a marked suppression of activity (Fig. 7B, lower left, periods 2 and 4). However, the activity of the knockout group was lower than that of the wild-type group [$F(1,15) = 4.89$, $P < 0.05$, repeated-measures ANOVA] (Fig. 7B, lower right).

When pentylenetetrazol was injected intraperitoneally at the dose of 50 mg/kg, no difference in susceptibility to seizures was observed between wild-type and knockout mice: seven out of eight animals from both genotypes had myoclonic seizures and two out of eight wild types and three out of eight knockouts had clonicotonic seizures.

DISCUSSION

Expression of RPTPγ was detected early during development in the nervous system as well as in other organs, including intestine, kidney, testis, stomach, thymus, and vasculature. Comparison of tissue anatomies of wild-type and RPTPγ-null mice by histology did not reveal any apparent alterations. In the nervous system, the lack of apparent defects in neuronal development during embryogenesis indicates that RPTPγ is not necessary for neural commitment. RPTPγ expression was not detected in adult brain cells where neurogenesis occurs, indicating that RPTPγ is not necessary for adult neurogenesis. The localization of RPTPγ in the brain shows expression primarily in neurons, an observation confirmed by the colocalization of β-Gal activity and the neuronal marker NeuN. RPTPγ is expressed particularly in cortical layers II and V, and we observed a higher density of labeled neurons in layer II, while in layer V they appeared more dispersed. This distribution is typical of the pyramidal neurons in both layers. Moreover, in the hippocampus, only the stratum pyramidale, containing the cell bodies of the pyramidal cells, is labeled. Neutral red staining and retrograde transport using dextran-biotin confirmed that RPTPγ is expressed in the pyramidal neurons. Although we cannot exclude that other neurons are labeled with β-Gal in the brain, the lack of labeling in the other part of the hippocampus suggests that interneurons are not a cell population expressing RPTPγ.

One interesting comparison is with the localization of RPTPζ (the second member of the family), which might have been presumed to compensate for the lack of expression of RPTPγ. However, in the CNS, RPTPζ is strongly expressed in glial cells, astrocytes and oligodendrocytes, and in only a subset of neurons (3, 7, 21). Moreover, it is detected primarily in the subventricular zone, the dentate gyrus, and some cells of the cortex. Thus, in the brain, RPTPγ and RPTPζ appear to be expressed in different cell types and in different parts of the brain, suggesting that these two related phosphatases have different functions.

While we did not detect expression of RPTPγ in quiescent cortical astrocytes, it has been shown recently that RPTPγ is upregulated in activated astrocytes (18). It was demonstrated that RPTPζ is upregulated in glial cells, including oligodendrocytes and astrocytes, following injury (6, 12, 13, 15, 22). This suggests that these two RPTP may have potentially overlapping roles in certain pathological conditions.

The Timm staining in the hippocampus did not show any apparent alteration in the development of the neurites and in branching. However, it has been reported that PC12D cells overexpressing RPTPγ-A show reduced NGF-induced neurite outgrowth (20). We prepared DRG explants from wild-type and RPTPγ-deficient E12.5 and E14.5 embryos and followed neurite outgrowth for 24 h after NGF addition. Whether cultured on collagen- or poly-D-lysine-coated dishes, DRG explants deficient in RPTPγ develop normally, demonstrating that RPTPγ is not required for NGF-induced neurite outgrowth.

Surprisingly, we did not detect any expression of RPTPγ in the motor neurons of the spinal cord, in contrast to what has been described for the chick (4). It has been shown that RPTPψ is also expressed differently in *Xenopus laevis*, the chick, and the mouse (4, 8, 23).

RPTPγ is localized in sensory organs, in particular, in the cells that transform or transmit external stimuli to chemical signals. These cells include the ganglion cells of the retina, the sensory cells of the ear, the papillae of the tongue, the vibrissae of the nose, and the olfactory cells. We do not know yet which type of molecules could be regulated by RPTPγ. Ion channels have been shown to be regulated by phosphorylation and by PTP. For example, PTPα (26) and PTPε (14) can regulate the activity of potassium channels, and RPTPζ has been described as regulating a sodium channel (16, 17). Further studies will be needed to test whether RPTPγ regulates similar signaling pathways in these different cells to accomplish such functions.

RPTPγ-null mice had normal circadian activity. Mutants displayed specific motor deficits in the rotarod and string tests and reduced latency to react in the tail flick test. Analysis of emotional behavior showed that knockout mice had levels of anxiety and despair behavior comparable to those of wild-type littermates. Cognitive tests revealed that mutant mice showed significant enhancement of sensory processing for acoustic stimuli and reduced performance with cued fear conditioning. Working memory performance and contextual fear response were comparable to levels for wild-type littermates. Finally, knockout mice did not show altered susceptibility to pentylenetetrazol-induced seizures.

The interpretation of the subtle behavioral changes is not simple. The deficits determined by the rotarod and string tests may reflect alterations in balance or motor coordination and in traction force. It is possible that alterations in the cranial nerve, particularly the one involved in the vestibulocochlear system, may partially account for these deficits. Similarly, the enhanced prepulse inhibition may involve alterations to this system. The differential sensitivities to pain, as measured by the tail flick and hot-plate tests, suggest that while the supraspinal response to pain is grossly normal, there are differences in the spinal responses, perhaps related to the expression of RPTPγ in the dorsal spine and the dorsal root ganglia.

In summary, we have carried out detailed expression and behavioral analyses of RPTPγ-null mice. RPTPγ is a member of a family of phosphatases that also includes RPTPζ. Yet, our study makes a clear demarcation between these two phosphatases, with RPTPγ showing expression in pyramidal and sensory neurons and RPTPζ showing expression in glial cells. Further characterization of RPTPγ knockouts in specific paradigms and in specific cells will lead to a better understanding of the regulatory role of this phosphatase. Furthermore, studies of nonneuronal cells and particularly of the colon, where RPTPγ appears to play a role in malignancies, are now feasible.

ACKNOWLEDGMENTS

We thank Ayala King and Patricia Gaspar for helpful suggestions as well as Muriel Lecocq and Aurore Bugi for excellent technical assistance.

This work was supported by grants to S.H. from the Federation pour la Recherche sur le Cerveau (FRC), l'Association pour la Recherche contre le Cancer (ARC), l'Association pour la Recherche contre la Sclerose en Plaque (ARSEP), GPH-Stem Cells of the Pasteur Institute (Paris, France), and Association Pasteur-Weizmann, as well as by grants from the Ludwig Institute for Cancer Research (to J.S.) and the NIH (RO1-AR051448 and RO1-AR051886 to J.S. and P50-MH066392 to J.D.B.). S. Lamprianou is a recipient of a fellowship from the French Ministry. N. Vacaresse was a recipient of an ELA (European Association against Leucodystrophy) fellowship.

REFERENCES

1. **Barnea, G., O. Silvennoinen, B. Shaanan, A. M. Honegger, P. D. Canoll, P. D'Eustachio, B. Morse, J. B. Levy, S. Laforgia, K. Huebner, J. M. Musacchio, J. Sap, and J. Schlessinger.** 1993. Identification of a carbonic anhydrase-like domain in the extracellular region of RPTPγ defines a new subfamily of receptor tyrosine phosphatases. Mol. Cell. Biol. **13:**1497–1506.
2. **Bixby, J. L.** 2001. Ligands and signaling through receptor-type tyrosine phosphatases. IUBMB Life **51:**157–163.
3. **Canoll, P. D., G. Barnea, J. B. Levy, J. Sap, M. Ehrlich, O. Silvennoinen, J. Schlessinger, and J. M. Musacchio.** 1993. The expression of a novel receptor-type tyrosine phosphatase suggests a role in morphogenesis and plasticity of the nervous system. Brain Res. Dev. Brain Res. **75:**293–298.
4. **Chilton, J. K., and A. W. Stoker.** 2000. Expression of receptor protein tyrosine phosphatases in embryonic chick spinal cord. Mol. Cell. Neurosci. **16:**470–480.
5. **Danscher, G., and J. Zimmer.** 1978. An improved Timm sulphide silver method for light and electron microscopic localization of heavy metals in biological tissues. Histochemistry **55:**27–40.
6. **Dobbertin, A., K. E. Rhodes, J. Garwood, F. Properzi, N. Heck, J. H. Rogers, J. W. Fawcett, and A. Faissner.** 2003. Regulation of RPTPbeta/phosphacan expression and glycosaminoglycan epitopes in injured brain and cytokine-treated glia. Mol. Cell. Neurosci. **24:**951–971.
7. **Harroch, S., M. Palmeri, J. Rosenbluth, A. Custer, M. Okigaki, P. Shrager, M. Blum, J. D. Buxbaum, and J. Schlessinger.** 2000. No obvious abnormality in mice deficient in receptor protein tyrosine phosphatase β. Mol. Cell. Biol. **20:**7706–7715.

7a. **Hatcher, J. P., D. N. Jones, D. C. Rogers, P. D. Hatcher, C. Reavill, J. J. Hanan, and A. J. Hunter.** 2001. Development of SHIRPA to characterise the phenotype of gene-targeted mice. Behav. Brain Res. **125:**43–47.

7b. **Irwin, S.** 1968. Comprehensive observational assessment. Ia. A systematic, quantitative procedure for assessing the behavioral and physiologic state of the mouse. Psychopharmacologia **13:**222–257.

8. **Johnson, K. G., and C. E. Holt.** 2000. Expression of CRYP-alpha, LAR, PTP-delta, and PTP-rho in the developing Xenopus visual system. Mech. Dev. **92:**291–294.
9. **Johnson, K. G., and D. Van Vactor.** 2003. Receptor protein tyrosine phosphatases in nervous system development. Physiol. Rev. **83:**1–24.
10. **Kastury, K., M. Ohta, J. Lasota, D. Moir, T. Dorman, S. LaForgia, T. Druck, and K. Huebner.** 1996. Structure of the human receptor tyrosine phosphatase gamma gene (PTPRG) and relation to the familial RCC t(3;8) chromosome translocation. Genomics **32:**225–235.
11. **LaForgia, S., B. Morse, J. Levy, G. Barnea, L. A. Cannizzaro, F. Li, P. C. Nowell, L. Boghosian-Sell, J. Glick, A. Weston, et al.** 1991. Receptor protein-tyrosine phosphatase gamma is a candidate tumor suppressor gene at human chromosome region 3p21. Proc. Natl. Acad. Sci. USA **88:**5036–5040.
12. **Maeda, N., H. Hamanaka, A. Oohira, and M. Noda.** 1995. Purification, characterization and developmental expression of a brain-specific chon-

droitin sulfate proteoglycan, 6B4 proteoglycan/phosphacan. Neuroscience **67:**23–35.

13. **McKeon, R. J., M. J. Jurynec, and C. R. Buck.** 1999. The chondroitin sulfate proteoglycans neurocan and phosphacan are expressed by reactive astrocytes in the chronic CNS glial scar. J. Neurosci. **19:**10778–10788.

13a. **Meziane, H., C. Mathis, S. M. Paul, and A. Ungerer.** 1996. The neurosteroid pregnenolone sulfate reduces learning deficits induced by scopolamine and has promnestic effects in mice performing an appetitive learning task. Psychopharmacology (Berlin) **126:**323–330.

14. **Peretz, A., H. Gil-Henn, A. Sobko, V. Shinder, B. Attali, and A. Elson.** 2000. Hypomyelination and increased activity of voltage-gated K^+ channels in mice lacking protein tyrosine phosphatase epsilon. EMBO J. **19:**4036–4045.

15. **Perosa, S. R., M. A. Porcionatto, A. Cukiert, J. R. Martins, C. C. Passeroti, D. Amado, S. L. Matas, H. B. Nader, E. A. Cavalheiro, J. P. Leite, and M. G. Naffah-Mazzacoratti.** 2002. Glycosaminoglycan levels and proteoglycan expression are altered in the hippocampus of patients with mesial temporal lobe epilepsy. Brain Res. Bull. **58:**509–516.

16. **Ratcliffe, C. F., Y. Qu, K. A. McCormick, V. C. Tibbs, J. E. Dixon, T. Scheuer, and W. A. Catterall.** 2000. A sodium channel signaling complex: modulation by associated receptor protein tyrosine phosphatase beta. Nat. Neurosci. **3:**437–444.

17. **Salter, M. W., and Y. T. Wang.** 2000. Sodium channels develop a tyrosine phosphatase complex. Nat. Neurosci. **3:**417–419.

18. **Schumann, G., B. L. Fiebich, D. Menzel, M. Hull, R. Butcher, P. Nielsen, and J. Bauer.** 1998. Cytokine-induced transcription of protein-tyrosine-phosphatases in human astrocytoma cells. Brain Res. Mol. Brain Res. **62:**56–64.

19. **Shintani, T., N. Maeda, T. Nishiwaki, and M. Noda.** 1997. Characterization of rat receptor-like protein tyrosine phosphatase gamma isoforms. Biochem. Biophys. Res. Commun. **230:**419–425.

20. **Shintani, T., N. Maeda, and M. Noda.** 2001. Receptor-like protein tyrosine phosphatase gamma (RPTPgamma), but not PTPzeta/RPTPbeta, inhibits nerve-growth-factor-induced neurite outgrowth in PC12D cells. Dev. Neurosci. **23:**55–69.

21. **Shintani, T., E. Watanabe, N. Maeda, and M. Noda.** 1998. Neurons as well as astrocytes express proteoglycan-type protein tyrosine phosphatase zeta/RPTPbeta: analysis of mice in which the PTPzeta/RPTPbeta gene was replaced with the LacZ gene. Neurosci. Lett. **247:**135–138.

22. **Snyder, S. E., J. Li, P. E. Schauwecker, T. H. McNeill, and S. R. Salton.** 1996. Comparison of RPTP zeta/beta, phosphacan, and trkB mRNA expression in the developing and adult rat nervous system and induction of RPTP zeta/beta and phosphacan mRNA following brain injury. Brain Res. Mol. Brain Res. **40:**79–96.

23. **Sommer, L., M. Rao, and D. J. Anderson.** 1997. RPTP delta and the novel protein tyrosine phosphatase RPTP psi are expressed in restricted regions of the developing central nervous system. Dev. Dyn. **208:**48–61.

24. **Sorio, C., P. Melotti, D. D'Arcangelo, J. Mendrola, B. Calabretta, C. M. Croce, and K. Huebner.** 1997. Receptor protein tyrosine phosphatase gamma, Ptp gamma, regulates hematopoietic differentiation. Blood **90:**49–57.

25. **Takahashi, T., R. S. Nowakowski, and V. S. Caviness, Jr.** 1996. Interkinetic and migratory behavior of a cohort of neocortical neurons arising in the early embryonic murine cerebral wall. J. Neurosci. **16:**5762–5776.

26. **Tsai, W., A. D. Morielli, T. G. Cachero, and E. G. Peralta.** 1999. Receptor protein tyrosine phosphatase alpha participates in the m1 muscarinic acetylcholine receptor-dependent regulation of Kv1.2 channel activity. EMBO J. **18:**109–118.

26a. **Wall, P. M., and C. Messier.** 2002. Infralimbic kappa opioid and muscarinic M1 receptor interactions in the concurrent modulation of anxiety and memory. Physicopharmacology (Berlin) **160:**233–244.

27. **Wang, Z., D. Shen, D. W. Parsons, A. Bardelli, J. Sager, S. Szabo, J. Ptak, N. Silliman, B. A. Peters, M. S. van der Heijden, G. Parmigiani, H. Yan, T. L. Wang, G. Riggins, S. M. Powell, J. K. Willson, S. Markowitz, K. W. Kinzler, B. Vogelstein, and V. E. Velculescu.** 2004. Mutational analysis of the tyrosine phosphatome in colorectal cancers. Science **304:**1164–1166.

28. **Wu, C. W., H. L. Kao, A. F. Li, C. W. Chi, and W. C. Lin.** Protein tyrosine-phosphatase expression profiling in gastric cancer tissues. Cancer Lett., in press.